

Research and Application of New Anti-CO₂ Pollution and Low Damage Water-based Drilling Fluid (ICCUSC2023)

Mingna Bai^{1,3}, Yonggang Xie^{1,3}, Haiyong Cheng^{2,3}, Yong Ouyang^{1,3}, Zhifeng Duan^{1,3}, Yunwen Gao^{1,3}, Zhijun Li^{1,3}, Shifu Yu^{1,3}, Yu Zhou^{1,3*}, Daichun Si^{1,3}, Jiangfeng Xie^{1,3}, Chunyu Cheng^{1,3}

1 Oil and Gas Technology Research Institute, ChangQing Oilfield Company, Xi'an, Shaanxi 710018, China

2 Engineering Technology Management Department, ChangQing Oilfield Company, Xi'an, Shaanxi 710018, China

3 National Engineering Laboratory of Low-Permeability Oil & Gas Exploration and Development, Xi'an, Shaanxi 710018, China

(*Corresponding Author: zhouyu_cq@petrochina.com.cn)

ABSTRACT

CO₂ intrusion into the drilling fluid during bauxite drilling can cause hydration swelling and dispersion of clays and lead to massive foaming of them. Additionally, the formation develops micro-nano fractures, which also have a large difference in compressive strength and a high percentage of bound water. Once the foreign fluid invades, it will lead to wellbore destabilization and reservoir damage. Thus, the designed drilling fluid formulation does not contain solid phase particles such as bentonite. And we obtained the optimal proportion of hydrolocker, penetrant, and defoamer by Mixture Designs. Then the shielding plugging theory was introduced, and a temporary plugging gradation consisting of acid-soluble inert particles, deformable nano-sealers, and non-permeable sealers was constructed with the aid of BridgePro software. And other surfactants were optimized indoors to build a low-damage, strong anti-CO₂ pollution water-based drilling fluid. It could resist the high temperature of 150°C and has a remarkable ability to lower surface tension (17.3mN). The rolling recovery, the plugging rate, and permeability recovery value can reach more than 90%, the lubrication coefficient was around 0.125. The constructed drilling fluid completed 9 wells in field application, with an obvious reservoir protection effect and an average increase of more than 20% in single-well daily production compared to the expected daily production. It will be an important reference for future bauxite horizontal well drilling fluids to prevent CO₂ contamination and reduce reservoir damage.

Keywords: CO₂ gas intrusion; Bauxite; Wellbore destabilization; Reservoir damage

NONMENCLATURE

Abbreviations

LCMs	lost circulation materials
PSD	particle-size distribution

1. INTRODUCTION

Bauxite is a rock group rich in aluminous minerals and dominated by chemical deposition with mechanical deposition characteristics^[1-3]. More recently, Changqing oilfield has obtained 67.38×10⁴ m³/d of high-yield industrial gas flow from the Longdong area of the Ordos Basin, achieving a breakthrough in a new unconventional gas reservoir in the Paleozoic bauxite of the basin^[4]. During the previous on-site drilling process, it was found that there was a high risk of gas intrusion of H₂S, CO, CO₂, and other gases.

Previous studies have shown that CO₂ intrusion into the drilling fluid during bauxite drilling can cause the hydration dispersion of clays and lead to massive foaming of them^[5, 6]. Furthermore, the presence of HCO₃⁻ can cause a significant decrease in the pH of the drilling fluid, failing some surfactants suitable for alkaline environments^[7, 8]. Additionally, the formation develops micro-nano fractures, which also have a large difference in compressive strength and a high percentage of bound water^[9, 10]. As the basic constituent of clays, Smectite and Illite of clay minerals are hydrated easily when they come in contact with water^[11, 12]. Due to the maturity of many bauxite formations, numerous microcracks are present and range from the nanometer to the micrometer level^[9]. The water infiltration will increase pore pressure and thereby reduce the mechanical strength of bauxite. Inevitably, due to the high-bound water in the bauxite,

water lock damage develops around the bauxite pore throat. Therefore, it is particularly important to effectively prevent CO₂ intrusion, wellbore collapse, and reservoir damage during the drilling process.

In response to the contamination caused by CO₂ intrusion into the drilling fluid, it has been shown that reducing the solid phase content in the drilling fluid is a good option^[5, 7]. And the drilling fluid in an alkaline environment neutralizes some of the HCO₃⁻, to ensure the stable rheological properties of the drilling fluid. In addition, the incorporation of a defoamer can reduce the foam generated by the drilling fluid after CO₂ intrusion.

Regarding Bauxite pore throats, it is an excellent approach that nanoparticles were adopted to prevent filtrate invasion to formation for reducing permeability and plugging nano-micron pore throats^[13-15]. In recent decades, various plugging additives have been developed such as nanoparticles, deformable particles, latex particles, aluminum complexes, additives based on modified Fe₃O₄ nanoparticles, nano-cellulose category, solid particles include SiO₂, TiO₂ or ZnO, etc^[16-18]. It is worth noting that the size distribution of LCMs is one of the most important factors in plugging performance^[19]. Some pioneering work has been done on bridging theories involving the relationship between the PSD of bridging particles and the size distribution of pore throats in the rock^[20, 21]. These plugging theories mainly include the maximum density theory, the ideal packing theory, the shielding temporary plugging theory, the one-third rule, the two-thirds rule, the D₉₀ rule, and the ideal packing baseline method, etc^[21-23].

Owing to the excellent surface tension reduction ability of surfactants, organosilicon fluorinated and nonionic surfactants have been widely applied^[10, 24]. In particular, the penetrant itself has a fixation effect, so as to orient the hydrophilic and lipophilic groups on the water surface and further reduce the surface tension. However, too low a surface tension in the drilling fluid filtrate can lead to foaming^[25, 26]. Therefore, a certain amount of defoamer must be added to maintain the stability of the drilling fluid^[25].

In this paper, bentonite was removed from the conventional water-based drilling fluid formulation to reduce the contamination of drilling fluid by CO₂. Subsequently, the optimal ratio of hydro-locker, permeation agent, and defoamer was optimized by Mixture Designs to improve the reservoir protection performance of drilling fluid, thus significantly reducing the hydro-lock damage and foaming phenomenon. In order to improve the wellbore stability, a three-stage temporary plugging grade consisting of acid-soluble inert

particles, and deformable and non-permeable pluggings was constructed with the aid of BridgePro software to enhance the plugging ability of the drilling fluid. Finally, the types and dosages of flow regulators, inhibitors, and lubricants were selected to develop an anti-CO₂ pollution and low-damage water-based drilling fluid for bauxite horizontal wells based on field drilling fluids.

2. MATERIAL AND METHODS

2.1 Materials

All the bauxite samples with different burial depths were taken from the Long 74 well in China Ordos Basin. Deionized water, and saturated brine (26.47%) were provided by Aladdin Reagent Co., Ltd., Shanghai, China. Hydrolockers SSF (99.9%) came from Shanghai Kolaman Reagent Co., Ltd, China. FC-1, JY-1, JFC, and GS were all analytical and provided by China Beijing Inokai Technology Co., LTD. Na₂CO₃, CAB-35, SDS, BS-12, CTAC, ABS, and hydrophobic silica nanoparticles were all analytical and obtained from Xinbaohai Chemical Technology Co., Ltd., China. The 1250 mesh calcium carbonate particles were purchased from Yanan Chaozheng Mud Company Limited, China. The nano-nonpermeable plugging agent NP-1 ($D_{50} \leq 0.9\mu\text{m}$) and the deformable nano-plugging DWF-1 ($FL_{HTHP,150^\circ\text{C} \times 3.5\text{MPa}} \leq 35.0\text{mL}$) were provided by China Shandong Deshunyuan Petroleum Technology Co.

2.2 Methods

2.2.1 Experimental method of bauxite properties

2.2.1.1 Physicochemical performance

The rock samples of the bauxite reservoir were analyzed by X-ray diffractometer for mineral composition. Then the hydration and dispersion properties were evaluated by XGRL-4A digital roller heating furnace and CST tester. These two experimental steps were completed by referring to the Chinese industry standards NB/T 10121-2018 and SY/T 5163-2018 turn.

2.2.1.2 Microstructural analysis

First, the bauxite of the Long 74 well was processed to remove the impurities on the surface, then dried at room temperature for 48 h, and then cut into 0.5 cm² × 0.5 cm² cubes. The prepared portion of the rock samples has adhered to a metal disk of conductive tape, then metal sprayed for 20 min and finally used for testing with SEM5000.

2.2.1.3 Mechanical properties

Deionized water and saturated brine were utilized to soak the bauxite at a depth of 4228.05m in the reservoir

for 15 days. And then the mechanical properties were evaluated using China XULIAN multifunctional rock pressure tester. And this experiment is a reference to Chinese corporate standards Q/SY 02020-2017.

2.2.1.4 Bound water distribution

MRI NMR was adopted to analyze the distribution pattern of bound water in the pore throat of bauxite at different burial depths. And the experimental method follows the Chinese petroleum industry standard SY/T 6490-2007.

2.2.2 Optimization of hydro-locking agents

2.2.2.1 Determination of surface tension

A JC2000C1 contact angle measuring instrument was adopted to evaluate the surface tension reduction ability of different hydrolockers. A microsyringe was used to obtain the solution prepared by them. When the sample in the syringe formed a droplet at the end of the syringe needle and the droplet approached the maximum diameter, the droplet image was saved. The droplet image was processed by software to obtain the surface tension value of the agents.

2.2.2.2 Preparation of solutions

Refer to China Petroleum Industry Standard SY/T 5350-2009, a specification for evaluating hydrolockers for drilling fluids. The experiment was selected to conduct under room temperature (25°C). The hydrolocking agent of a specific concentration was then added with 100 mL water and stirred the aqueous solution via 11000r/min for 1 min. Next, the aqueous solution was immediately poured into a 500 mL graduated cylinder while starting timing and recording the maximum foam volume V_m of the initial foam. Finally, the percentage of the generated foam in the aqueous solution was calculated.

2.2.2.3 Mixing optimization experiments

The mixing optimization method can reduce the number of experiments, and study the interaction between several design factors. In contrast, orthogonal experiments can only analyze isolated experimental points. Thus, the mixing optimization method was performed to optimize the surface tension, which was used as the evaluation index to optimize the concentration of different desiccant lockers. Moreover, the total percentage of their dosage added during the experiment was maintained at 0.5%.

2.2.3 Optimization of plugging additives

2.2.3.1 Optimization method

The results of scanning electron microscopy experiments indicated that the size of microfractures

developed in bauxite was 0~8 μm . Drawing on the theory of shielding temporary plugging^[27, 28], 1250 mesh calcium carbonate particles were introduced, which can form bridges at the rock pore throats. Then the nano-nonpermeable plugging agent NP-1 was utilized to further fill and reduce the permeability of the plugging zone. Finally, the deformable nano-plugging DWF-1 was introduced to seal the irregular micrographs still present in the pores.

The dosage of the three blocking agents was optimized by BridgePro from PVI. The particle size distribution characteristics were also analyzed by a Malvern Zetasizer nanoparticle size potentiostat.

2.2.3.2 Performance evaluation

Referring to Chinese Standard SY/T 5241-1991 evaluation procedures for water lossless agents for water-based drilling fluids, the plugging performance of formulation was measured in a high-temperature environment via a PPA high-temperature and high-pressure filtration apparatus. And the experimental conditions were set at 150°C×3.5MPa×30min. The experimental process started with the addition of the preferred plugging formulation to the field drilling fluid formulations without bentonite, followed by performance measurements. And the formulation of the on-site drilling fluid was 1.5% bentonite+0.1%Na₂CO₃+4%SMP+2%SFT+0.3%PAC-HV+1.0%AP-1+5.0%KCl+2.0%XCS-3.

2.2.4 Drilling fluid performance assessment

2.2.4.1 Preparation of the drilling fluid

After mixing experiment and BridgePro optimization to obtain the proportioning of hydrolocker and plugging agent, the formulation of the drilling fluid was determined. The composition of the formulation is that 4%SMP+2%SFT+0.3%PAC-HV+1.0%AP-1+5.0%KCl + 2.0%XCS-3+0.5% hydrolocker+6.0% plugging agent. Then, the drilling fluid treatment agents were added to 900 ml of water at room temperature (25°C), respectively. And the suspension was stirred at 8000r/min for 30 minutes to obtain the drilling fluid sample.

2.2.4.2 Evaluation of the performance of drilling fluid

First, we divided the prepared drilling fluid (900mL) into nine groups and numbered each of them. The evaluation performance of drilling fluid mainly included five parts: CO₂ pollution resistance, plugging performance, suppression performance, reservoir protection performance, and lubricity performance. Read Table 1 for the relevant evaluation standards of drilling fluid performance.

Table 1 Stands for the determination of various performances of drilling fluid

Measurement performance	National, petroleum industry and enterprise standards
CO2 pollution resistance	GB/T 16783.1-2014 Water-based drilling fluid field test steps
Plugging performance	Q/SY/ 5840-2007 China's petroleum enterprise -standard Indoor test method for drilling fluid bridging and plugging materials
Suppression performance	SY/T5613-2000 China's petroleum industry-standard Mud shale's physical and chemical properties
Reservoir protection performance	SY/T 6540-2002 China's petroleum industry-standard China's lab testing method of drilling and completion fluids damaging oil formation
Lubricity performance	SY/T 6094-1994 China's petroleum industry-standard Evaluation procedures for lubricants for drilling fluids

Table 2 XRD analysis of bauxite mineral compositions.

Mineral	Depth(m)	Quartzz(%)	Potassium feldspar(%)	Aluminite(%)	Anatase(%)	Clay(%)
Bauxite	4045.60	0.6	0	96.1	0	4.3
	4229.08	0	0.6	90.1	2.5	6.8

Table 3 Clay mineral compositions of bauxite.

Mineral	Depth(m)	Kaolinite(%)	Chlorite(%)	Elysium(%)	I/Mon interlayer(%)	Interlayer ratio (%)
Bauxite	4045.60	0	1	60	39	20
	4229.08	0	7	61	32	20

3. RESULTS AND DISCUSSION

3.1 Bauxite properties

3.1.1 Clay mineral compositions

The XRD analysis results of bauxite samples were shown in Tables 2 and 3, accordingly. The bauxite samples are mainly hydrous alumina with a small percentage of clay minerals. The clay minerals of bauxite samples are mainly illite (average 60.5%), followed by I/M interlayer (average 35.5%), and the interlayer ratios are both 20%, indicating that the stratigraphic rocks have some weak hydrated swelling characteristics.

3.1.2 Clay mineral compositions

The experimental results of hydration dispersion performance are presented in Figure 1. The primary and secondary rolling recoveries under clear water environment were above 80%, and the average absorption time of CST capillary was 12.77s, indicating the weak hydration dispersion of rock samples from bauxite reservoirs.

3.1.3 Microstructure of bauxite

The test results were displayed in Figure 2. The analysis indicated that the bauxite is developed with dissolution holes (<1μm), microporous fractures, interlayer fractures, etc. The size of microfractures in the rock sample is mainly within 0~8μm, and there is a

potential risk of leakage during drilling, which should focus on improving the plugging ability to drill fluid.

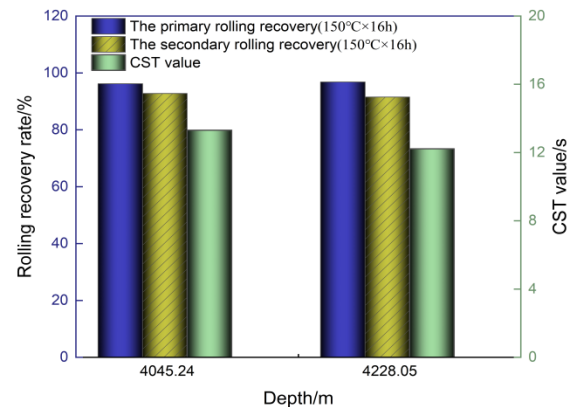


Fig. 1. Bauxite recovery experiments and CST test results

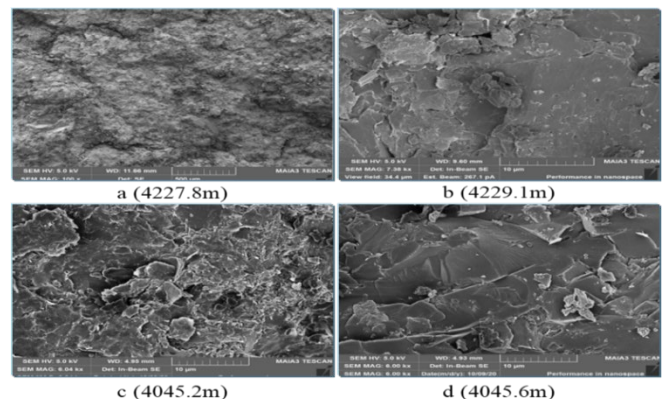


Fig. 2. Scanning electron micrograph of bauxite

Table 4 Mechanical performance results

Number	Surrounding pressure/ MPa	Length/ cm	Diameter/ cm	Poisson ratio	coefficient of restitution/ MPa	Compressive strength/ MPa	Note
1#	40.8	5.028	2.477	0.27	42528	149.27	dry
2#	40.8	5.005	2.477	0.46	20014	49.83	deionized water
3#	40.8	5.025	2.477	0.52	19846	48.75	saturated brine

3.1.4 Mechanical properties of bauxite

As shown in Fig.3 and Table 4, the compressive strength of the rocks was significantly weakened after 15 days of immersion in different media. The compressive strength of the rock was reduced by 66.61% and 67.34% after clear water and saturated brine soaking, respectively. It indicated that the intrusion of foreign fluids in the reservoir will reduce the mechanical strength of the rock and cause wellbore collapse.



Fig. 3. (a) Photographs of bauxite before soaking
(b) Photographs of bauxite after soaking for 15 days

3.1.5 Bound water distribution

The experimental results are presented in Figure 4. Overall the left peak (bound water) of all rock samples was much stronger than the right peak (movable water), and the percentage of bound water in the saturated water of cores was all up to more than 90%. It reveals that the fluid endowment state is mainly bound water state, so the main factor causing reservoir damage may be water lock damage^[29-31].

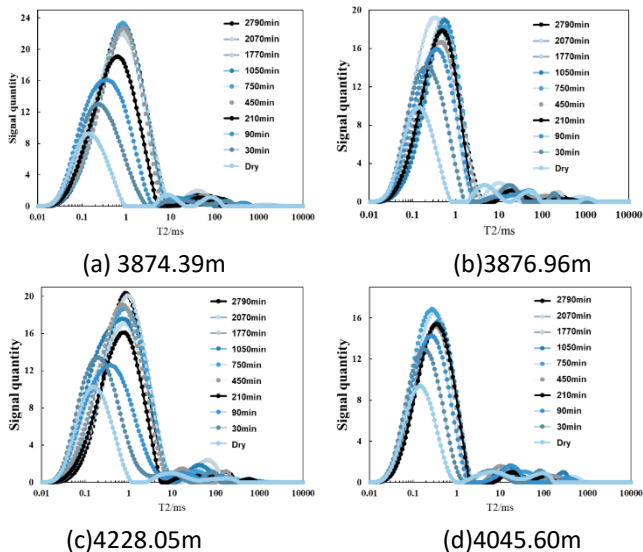


Fig. 4. T2 imbibition test results of different bauxite rocks

3.2 Optimization of hydrolocking agents

3.2.1 Category preference

The evaluation results are shown in Table 5. The detergent SSF, penetrant JFC, and defoamer GS have weak foaming performance and low surface tension (<25mN/m). It was attributed to the fact that SSF fluorine atoms are electronegative and have high ionization energy and oxidation potential, which can reduce the fluid surface tension^[32, 33]. Furthermore, the oriented arrangement of hydrophilic and lipophilic groups in the molecular structure of JFC on the fluid surface can reduce the core-bound water saturation^[34, 35]. Defoamer GS can inhibit the foaming of the solution and improve the effect of unlocking water. These three surfactants provide a synergistic effect to unlock the water^[25, 36].

Table 5 Experimental design and results.

Category	Aqueous solution	Surface tension /mN/m	Foaming rate /%
Organosilicon fluorine	0.5%SSF	20.72	6.8
	0.5%FC-1	26.45	6.5
	0.5%JY-1	31.89	5.2
Nonionic	0.5%JFC	23.56	4.8
	0.5%GS	27.28	1.6
Anionic	0.5%SDS	36.83	8.5
	0.5%ABS	49.92	6.5
	0.5%BS-12	48.69	9.0
Amphoteric ionic	0.5%CAB-35	56.45	7.2
	0.5%CTAC	55.72	6.8
Hydrophobic solid particles	0.5% nanoparticles	76.33	0.5

3.2.2 Mixing optimization experiments

Based on the Mixture Designs design principle, the dosage of SFF, JFC, and GS was optimized using surface tension as the evaluation index. The experimental design and results are presented in Table 6 and Figure 5. It

Table 6 Mixing experimental design and results

Number	A	B	C	Surface tension /mN/m
	GS/%	JFC/%	SFF/%	
1	26.5	73.5	0.0	47.3
2	69.0	12.8	18.2	36.5
3	0.1	49.8	50.1	32.4
4	100.0	0.0	0.0	50.8
5	49.7	0.0	50.3	25.6
6	100.0	0.0	0.0	46.5
7	21.3	7.4	71.3	17.5
8	50.4	48.8	0.8	46.4
9	50.4	48.8	0.8	42.8
10	0.0	0.0	100.0	21.6
11	1.8	73.5	24.6	40.5
12	49.7	0.0	50.3	24.2
13	0.0	100.0	0.0	46.0
14	32.7	32.5	34.8	38.7
15	32.7	32.5	34.8	38.5
16	0.1	49.8	50.1	30.4

Note: Surface tension = 48.5A + 46.67B + 21.53C - 11.49AB - 40.51AC - 11.63BC - 132.02A²B + 1412.05AB²C - 642.60ABC²; R² = 0.9827; Adj R² = 0.9629

indicates that the equations were fitted with high accuracy and experimental confidence (R² = 0.9827 and Adj R² = 0.9629). Among the interactions, the interaction of the antifoam agent SFF (A) and the defoamer GS (C) was extremely significant for the surface tension. And the lowest surface tension could be obtained when the percentage of GS, JFC, and SFF reached 21.3%, 7.4%, and 71.3, respectively.

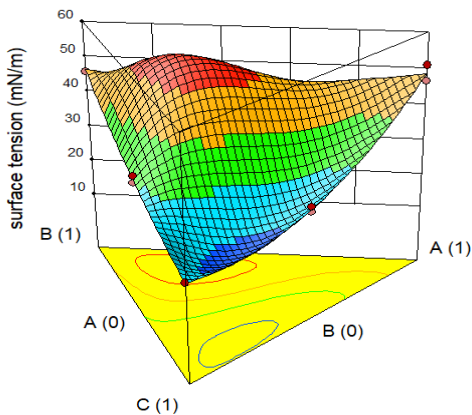


Fig. 5. Interaction effect of SFF, JFC, and GS addition on surface tension

3.3 Optimization of plugging formulations

3.3.1 Optimization results

The results of the ratios of the three plugging agents are presented in Figure 6a. The percentages of calcium carbonate particles, NP-1, and DWF-1 are 50.4%, 23.7%, and 25.9%, respectively. The results of the particle size distribution evaluation are shown in Figure 6b. The

particle size distribution of this plugging formulation ranges from 0.01 to 10 μm, and the median particle size is 4.47 μm, which indicates that the plugging formulation can effectively seal the microfractures in the bauxite formation.

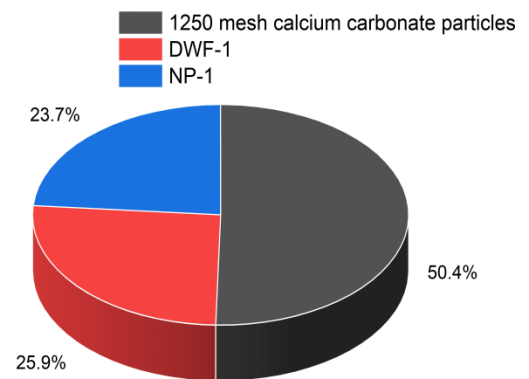


Fig. 6. (a) Design results of the optimal plugging formulation

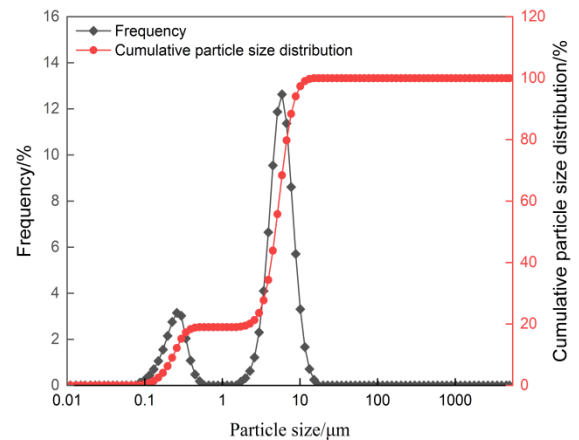


Fig. 6. (b) Design results of the optimal plugging formulation

Table 7 Comparison of drilling fluid performance against CO₂ contamination

Number	Experimental condition	$\rho/g/cm^3$	PV/mPa·s	AV/mPa·s	YP/Pa	YP/PV	FLHHP/mL	pH
On-site drilling fluids	Before aging,	1.40	27.0	41.0	14.0	0.52	15.0	9.0
	After aging	1.35	27.0	38.5	11.5	0.43	20.0	8.5
On-site drilling fluids+1.0%Na ₂ CO ₃	Before aging,	1.40	30.0	43.0	15.0	0.50	14.4	7.0
	After aging	1.41	28.0	39.5	11.5	0.41	25.2	7.0
On-site drilling fluids+3.0%Na ₂ CO ₃	Before aging,	1.40	39.0	56.0	17.0	0.44	38.6	6.5
	After aging	1.41	38.0	53.5	15.5	0.40	45.4	6.0
Anti-CO ₂ pollution and low-damage drilling fluid	Before aging,	1.20	18.0	43.0	25.0	1.39	4.5	9.5
	After aging	1.21	18.0	38.5	20.5	1.14	5.5	9.5
Anti-CO ₂ pollution and low damage drilling fluid+1.0% Na ₂ CO ₃ +Barite	Before aging,	1.40	24.0	53.0	29.0	1.21	6.0	9.5
	After aging	1.40	27.0	47.0	20.0	0.74	6.4	9.0
Anti-CO ₂ pollution and low damage drilling fluid+3.0% Na ₂ CO ₃ +Barite	Before aging,	1.40	28.0	48.5	20.5	0.73	6.6	9.0
	After aging	1.39	22.0	41.0	19.0	0.86	7.0	8.5
Anti-CO ₂ pollution and low damage drilling fluid+5.0% Na ₂ CO ₃ +Barite	Before aging,	1.50	40.0	62.5	22.5	0.56	18.8	8.0
	After aging	1.49	42.0	65.5	23.5	0.55	21.2	7.5

Note: Hot-rolling experiment:150°C×16h; Filtration loss experiment in high temperature and pressure: 150°C×3.5MPa×30min.

3.3.2 Performance evaluation

The results of the plugging performance tests at different dosages were shown in Fig.7. The instantaneous volume of FL_{HHP} can be reduced to 4.5 mL at a dosage greater than 6.0%. Satisfactorily, the reduction of the instantaneous plugging property was up to 72.5%. It demonstrated that the preferred combination of plugging agents can better plug pores and microfractures of different sizes. Thus, it can effectively carry out instantaneous plugging and play a role in stabilizing the wellbore.

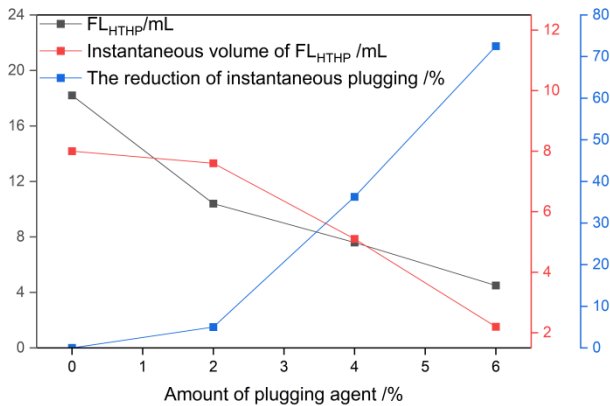


Fig. 7. Plugging performance evaluation results

3.4 Performance assessment of formulation

After mixing experiment and BridgePro optimization to obtain the proportioning of hydrolocker and plugging agent, the composition of the formulation is that 4% SMP + 2% SFT + 0.3% PAC-HV + 1.0% AP-1 + 5.0% KCl + 2.0% XCS-3 + 0.5% hydrolocker + 6.0% plugging agent. Among them, the hydrolocker SSF:JFC:GS=71.3%:7.4%:21.3%, and the plugging agent CaCO₃:NP-1: DWF-1 = 50.4%:23.7%:25.9%.

The experimental results of CO₂ pollution resistance were shown in Table 7. The viscosity and shear of the field drilling fluid increase accordingly, and the volume of water loss increased rapidly with the incorporation of CO₃²⁻. It indicated that the upper limit of CO₂ pollution resistance of the field composite salt drilling fluid was 1.0%. However, the upper limit of CO₂ contamination resistance of anti-CO₂ pollution and low damage drilling fluid has been increased to 3.0%, which proves its good resistance to contamination.

3.4.2 Plugging performance

Different sizes of rock slabs from 500mD-6700mD were selected to evaluate the plugging performance of drilling fluid by a PPA permeability plugging tester, and

the experimental results were presented in Figure 8. Under different rock slab conditions, the filtration loss of drilling fluid ($150^{\circ}\text{C} \times 3.5\text{MPa} \times 30\text{min}$) was less than 10mL, indicating that it can form high-quality mud cake quickly, achieve dense plugging and improve the stability of the wellbore.



Fig. 8. (a) Pictures of plugging of 6700mD rock slab

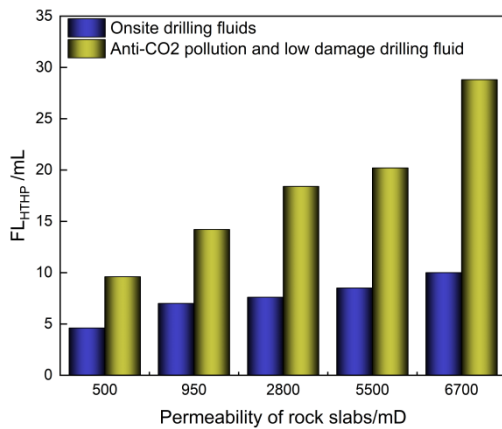


Fig. 8. (b) Results of filter loss of different rock slabs

3.4.3 Suppression performance

The bauxite at a burial depth of 4229.08m was selected for the experiment. And the inhibition performance of drilling fluid under a high-temperature environment of 150°C was evaluated by utilizing XGRL-4A digital roller heating furnace and HTTP-C4 high-temperature and high-pressure shale expander. The experimental results are shown in Figure 9. The primary and secondary rolling recovery rates of drill cuttings after adding drilling fluid were as high as 98.46% and 95.02%, respectively. The linear expansion of cuttings under high temperature and pressure conditions was only 0.164 mm. It was reduced by 1.663 mm and 1.092 mm compared to the deionized water and field drilling fluids, respectively. It indicated that the constructed drilling fluid has good inhibition and can significantly improve the stability of the wellbore.

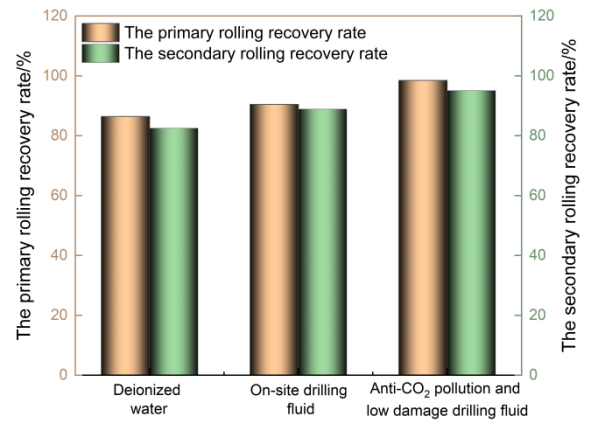


Fig. 9. (a) Results of heat roll recovery experiments

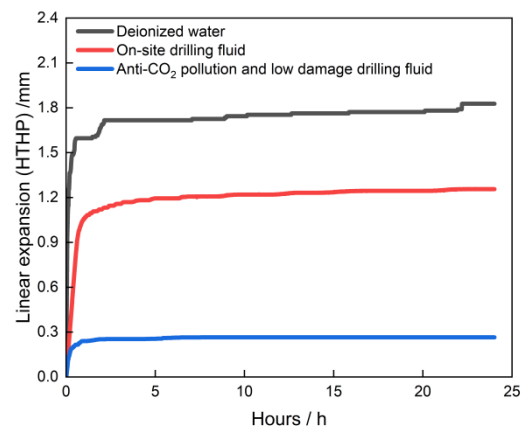


Fig. 9. (b) Linear expansion test results at high temperature and pressure

3.4.4 Reservoir protection performance

The reservoir protection performance of the drilling fluid was evaluated through the LDY50-180A core flow meter and the JC2000C1 contact angle measuring instrument. The experimental results were presented in Table 8, and the plugging rate and permeability recovery rate of the anti-CO₂ pollution and low-damage drilling fluid on the core (4229.08m) were up to more than 90%. In addition, the surface tension of the filtrate was reduced by 68.1% compared with that of the field drilling fluid. It indicated that the constructed drilling fluid had good reservoir protection.

3.4.5 Lubrication performance evaluation

The LEM-4100 high-temperature and high-pressure dynamic lubricator were selected to evaluate the lubricity of the anti-CO₂ pollution and low-damage drilling fluid, and the experimental results were presented in Table 9. The lubrication coefficient of the

Table 8 Evaluation results of reservoir protection performance

Categories	$K_1/10^{-3}\mu\text{m}^2$	$K_2/10^{-3}\mu\text{m}^2$	$K_3/10^{-3}\mu\text{m}^2$	Plugging rate/%	Recovery rate/%	Surface tension/mN
On-site drilling fluid	3.2333	0.4612	2.8081	85.7	86.9	54.2
Anti-CO ₂ pollution and low-damage drilling fluid	3.2718	0.2154	2.9958	93.4	91.6	17.3

Note: K_1 : Initial penetration; K_2 : Permeability after plugging; K_3 : The permeability measured after cutting the core end face by 5 mm and then reversing the replacement.

Table 9 Evaluation results of lubrication performance of drilling fluids at high temperature and pressure

Categories	Friction coefficient	Torque/in-lbs
On-site drilling fluid	0.162	31.2
Anti-CO ₂ pollution and low-damage drilling fluid	0.125	21.8

Note: Contact force 50 psi, pressure 3.5 MPa, temperature 150°C.

drilling fluid was 0.125, which was 22.8% lower compared with the field drilling fluid. It indicated that the drilling fluid can effectively reduce the friction of drilling tools and prevent complex accidents such as mud packs and stuck drilling in the downhole.

3.4.6 Field Experiment

Up to now, the anti-CO₂ pollution and low-damage drilling fluid have been applied to 9 wells in the field, and there were no complicated accidents such as wellbore collapse during the drilling process. In particular, the actual production capacity of a single well has increased by more than 20% compared with the expected original production capacity (Fig.10). It proves the advantages of the technical performance of this drilling fluid, which not only can safely complete the drilling target but also has obvious reservoir protection effect.

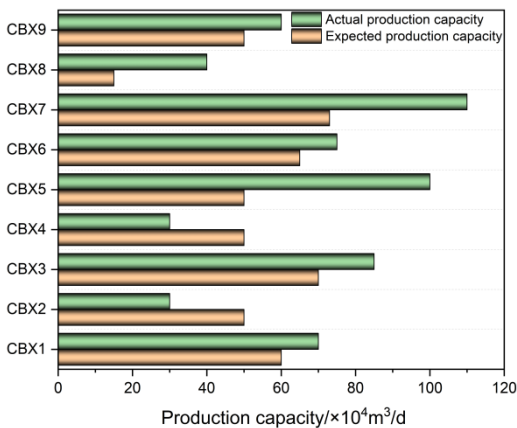


Fig. 10. Single well capacity profile in the late field test

4. CONCLUSIONS

(1) Bauxite rocks are developed with microporosity, and there is a large difference in the compressive strength of the rocks. During the drilling process, there is not only the risk of leakage but also the risk of foreign

fluids intruding into the formation and causing the reduction of the cementation strength of the Imon interlayer. Eventually, the bauxite will collapse and become unstable.

(2) Since the fluid endowment state in bauxite saturated water is mainly bound water. Once the reservoir is invaded by foreign fluids, it is prone to form a hydrolock and cause serious reservoir damage.

(3) The constructed drilling fluid was able to resist 3.0% CO₂ contamination. Moreover, the drilling fluid has remarkable surface tension reduction ability (17.3mN), and the rolling recovery rate, plugging rate, and permeability recovery value of bauxite were all over 90%, which has good plugging performance and reservoir protection performance. And the actual production capacity of a single well has increased by more than 20% compared with the expected original production capacity.

ACKNOWLEDGEMENT

This work was financially supported by the 2021 Exploration Tackling Project of CNPC, "Research on Drilling and Completion Technology of Tight Oil and Gas Horizontal Wells and Mid-Depth Wells on the Western Margin". [Project No. 22102-02-09].

DECLARATION OF INTEREST STATEMENT

The authors declare that they have no known competing financial interests or personal relationships that could have appeared to influence the work reported in this paper. All authors read and approved the final manuscript.

REFERENCE

[1] Cao JY, Wu QH, Li H, Ouyang CX, Kong H, Xi XS. Metallogenic mechanism of Pingguo bauxite deposit, western Guangxi, China: Constraints from REE geochemistry and multi-fractal characteristics of major

elements in bauxite ore. *JOURNAL OF CENTRAL SOUTH UNIVERSITY*. 2017;24:1627-36.

[2] Dodoo D, Appiah G, Acquah G, Junior TD. Fixed-bed column study for the remediation of the bauxite-liquid residue using acid-activated clays and natural clays. *Heliyon*. 2023;9:e14310.

[3] Liu L, Liu X, Yang S, Zhao L, Sun X, Zhang J. Mineralogical and geochemical investigations on the Early Permian Yuxi karstic bauxite deposit, Central Yunnan, China. *Ore Geology Reviews*. 2023;153:105296.

[4] Fu J, Li M, Zhang L, Cao Q, Wei X. Breakthrough in the exploration of bauxite gas reservoir in Longdong area of the Ordos Basin and its petroleum geological implications. *Natural Gas Industry*. 2021;41:1-11.

[5] Geng J, Yan J, Cao M, Bai X, Shi H. Scale deposition mechanism and low-damage underbalanced drilling fluids for high CO₂ content gas reservoirs. *Shiyou Kantan Yu Kaifa/Petroleum Exploration and Development*. 2011;38:750-5.

[6] Li XC, Kang YL. Effect of fracturing fluid immersion on methane adsorption/desorption of coal. *JOURNAL OF NATURAL GAS SCIENCE AND ENGINEERING*. 2016;34:449-57.

[7] Nie S, Feng B, Liu S, Sun X, Zhang X, Li B, et al. Technical measures for improving compatibility of cement slurry with CO₂ contaminated drilling fluid: A case study. *Natural Gas Industry*. 2013;33:91-6.

[8] Qin C, Jiang Y, Zhou J, Song X, Liu Z, Li D, et al. Effect of supercritical CO₂ extraction on CO₂/CH₄ competitive adsorption in Yanchang shale. *Chemical Engineering Journal*. 2021;412:128701.

[9] Rana A, Saleh TA, Arfaj MK. Nanosilica modified with moringa extracts to get an efficient and cost-effective shale inhibitor in water-based drilling muds. *Chemical Engineering and Processing - Process Intensification*. 2021;168:108589.

[10] Muhammed NS, Olayiwola T, Elkhatny S, Haq B, Patil S. Insights into the application of surfactants and nanomaterials as shale inhibitors for water-based drilling fluid: A review. *Journal of Natural Gas Science and Engineering*. 2021;92:103987.

[11] Abdullah AH, Ridha S, Mohshim DF, Yusuf M, Kamyab H, Krishna S, et al. A comprehensive review of nanoparticles: Effect on water-based drilling fluids and wellbore stability. *Chemosphere*. 2022;308:136274.

[12] Keshavarz Moraveji M, Ghaffarkhah A, Agin F, Talebkeikhah M, Jahanshahi A, Kalantar A, et al. Application of amorphous silica nanoparticles in improving the rheological properties, filtration and shale stability of glycol-based drilling fluids. *International*

Communications in Heat and Mass Transfer. 2020;115:104625.

[13] Gautam S, Guria C, Rajak VK. A state of the art review on the performance of high-pressure and high-temperature drilling fluids: Towards understanding the structure-property relationship of drilling fluid additives. *Journal of Petroleum Science and Engineering*. 2022;213:110318.

[14] Al-Shargabi M, Davoodi S, Wood DA, Al-Musai A, Rukavishnikov VS, Minaev KM. Nanoparticle applications as beneficial oil and gas drilling fluid additives: A review. *Journal of Molecular Liquids*. 2022;352:118725.

[15] Xu J-g, Qiu Z-s, Zhao X, Zhong H-y, Li G-r, Huang W-a. Synthesis and characterization of shale stabilizer based on polyethylene glycol grafted nano-silica composite in water-based drilling fluids. *Journal of Petroleum Science and Engineering*. 2018;163:371-7.

[16] Kamali F, Saboori R, Sabbaghi S. Fe₃O₄-CMC nanocomposite performance evaluation as rheology modifier and fluid loss control characteristic additives in water-based drilling fluid. *Journal of Petroleum Science and Engineering*. 2021;205:108912.

[17] Sadeghalvaad M, Sabbaghi S. The effect of the TiO₂/polyacrylamide nanocomposite on water-based drilling fluid properties. *Powder Technology*. 2015;272:113-9.

[18] Oseh JO, Mohd NMNA, Gbadamosi AO, Agi A, Blkoor SO, Ismail I, et al. Polymer nanocomposites application in drilling fluids: A review. *Geoenergy Science and Engineering*. 2023;222:211416.

[19] Razavi O, Karimi Vajargah A, van Oort E, Aldin M, Govindarajan S. Optimum particle size distribution design for lost circulation control and wellbore strengthening. *Journal of Natural Gas Science and Engineering*. 2016;35:836-50.

[20] Kumar A, Samuel R. Analytical Model to Characterize "Smear Effect" Observed While Drilling With Casing. *JOURNAL OF ENERGY RESOURCES TECHNOLOGY-TRANSACTIONS OF THE ASME*. 2014;136.

[21] Li ZY, Zhou Y, Qu L, Wang Y, Zhang SS. A New Method for Designing the Bridging Particle Size Distribution for Fractured Carbonate Reservoirs. *SPE JOURNAL*. 2022;27:2552-62.

[22] Ismail NI, Lawrence E, Naz MY, Shukrullah S, Sulaiman SA. Role of particle size distribution of bridging agent for drilling mud on formation damage near wellbore. *MATERIALS TODAY-PROCEEDINGS2021*. p. S13-S7.

[23] Sun J, Bai Y, Cheng R, Lyu K, Liu F, Feng J, et al. Research progress and prospect of plugging technologies for fractured formation with severe lost circulation.

Petroleum Exploration and Development. 2021;48:732-43.

[24] Muhammed NS, Olayiwola T, Elkatatny S. A review on clay chemistry, characterization and shale inhibitors for water-based drilling fluids. *Journal of Petroleum Science and Engineering*. 2021;206:109043.

[25] Li Z, Zhou Y, Qu L, Li H, Huang T. CBM foam drilling fluid based on hydrophilic silica nanoparticles. *PETROLEUM SCIENCE AND TECHNOLOGY*. 2022;40:2639-58.

[26] Li Z, Zhou Y, Qu L, Zhang X. Smart plugging and low-damage foam drilling fluid technology for CBM drilling. *INTERNATIONAL JOURNAL OF OIL GAS AND COAL TECHNOLOGY*. 2023;32:103-25.

[27] Jiang W, Zhang J, Wang J, Peng S, Huang W, Wang G. SHIELDING AND TEMPORARY PLUGGING TECHNOLOGY AND APPLICATION IN THE BIANCHENG AREA OF NORTH JIANGSU PROVINCE. *Natural Gas Industry*. 2006;26:81-3.

[28] Liu DW, Kang YL, Liu QW, Lei DS, Zhang B. Laboratory Research on Fracture-Supported Shielding Temporary Plugging Drill-In Fluid for Fractured and Fracture-Pore Type Reservoirs. *JOURNAL OF CHEMISTRY*. 2017;2017.

[29] Wang CW, Su YL, Wang WD, Li L, Zhang LP, Wang TX. Water Blocking Damage Evaluation and Mitigation Method in Tight Gas Reservoirs. *ENERGY & FUELS*. 2022;36:10934-44.

[30] Lai N, Ye Z, Liu X, Yang J, Zhang J. IN-HOUSE STUDY ON WATER LOCKING DAMAGE OF TIGHT SAND GAS RESERVOIRS WITH LOW PERMEABILITY. *Natural Gas Industry*. 2005;25:125-7.

[31] Ke C, Wei Y, Zhang Q, Zhang X. Progress of water lock damage and water lock release technology in low permeability gas reservoir. *Applied Chemical Industry*. 2021;50:1613-7,21.

[32] Zhang C, Liu X, Bai X, Xue D, Sun H, Zhang J, et al. Water separation performance and mechanism of fluoro-silicone amphiphilic polymers in diesel oil-water emulsion system. *China Surfactant Detergent and Cosmetics*. 2017;47:197-201.

[33] Long Z, Chen Y, Cui C, Xu L, Zhang H. STUDY ON COMPOSITE VISCOSITY REDUCER OF LIGNOSULFONATE GRAFT COPOLYMER/ORGANIC SILICON - FLUORINE POLYMER. *Oil Drilling & Production Technology*. 2005;27:26-7.

[34] Guohua Z, Bing L, Fengcai HOU, Yewu BI. Impact of Penetrant Solution Water Lock Effect on Gas Desorption. *Science & Technology Review*. 2011;29:45-50.

[35] Sun H, Yang Z, Wang X, Sun G, Li Z. Study of the performance of organosilicon oligomer impregnating

agents applied on the reinforced concrete surface. *The Ocean Engineering*. 2016;34:93-9.

[36] Qiufeng AN, Kun GUO, Ge LI, Hao LI. Synthesis of polyether silicone and its application in defoamer. *Journal of Textile Research*. 2009;30:90-4.